Deng et al_Supplementary Figure 1

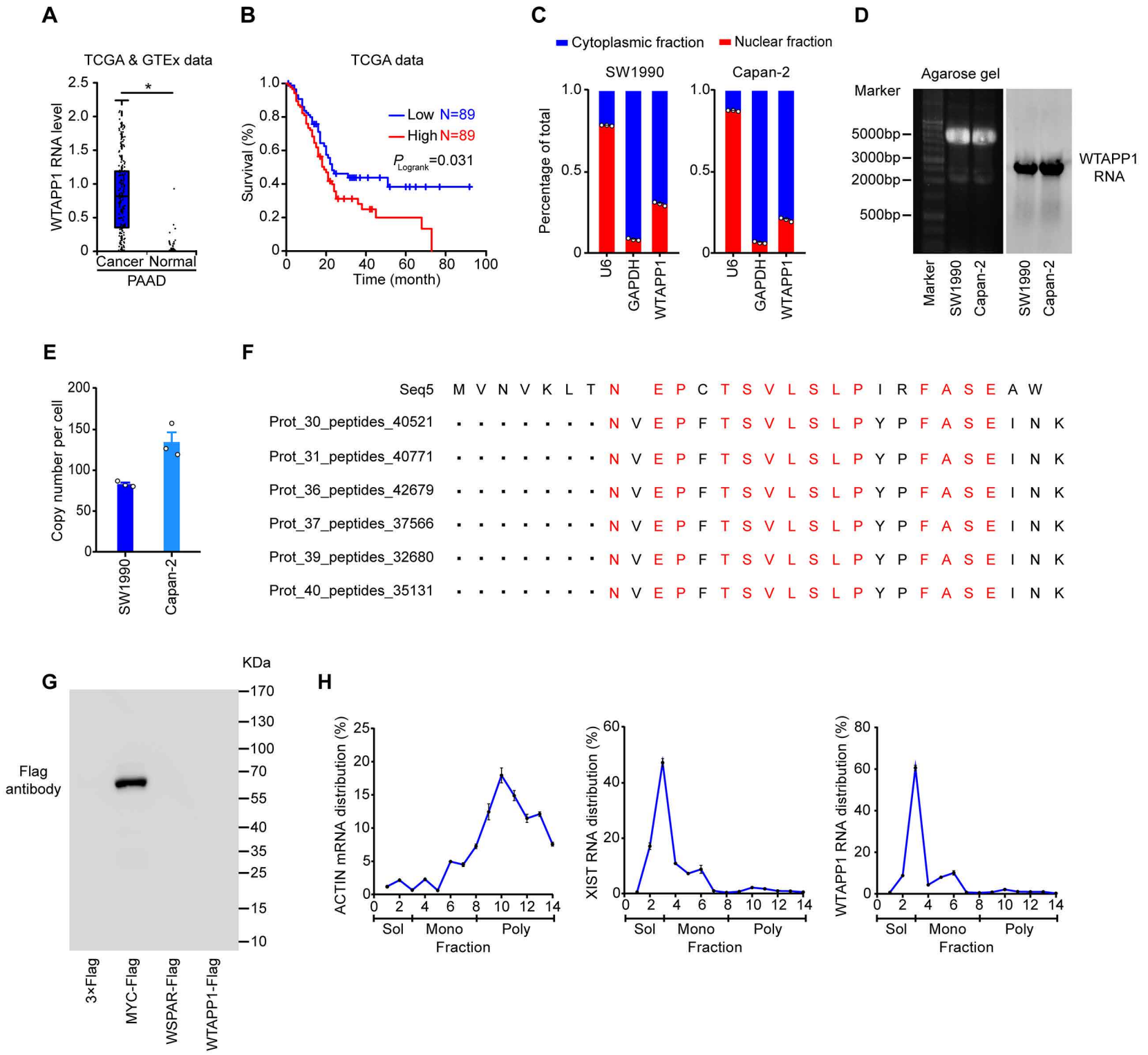

Supplementary Fig. S1 Additional Figures related to Fig. 1 (A) *WTAPP1* RNA levels in PDAC tumors (N = 179) compared with non-tumor tissues (N = 171) in TCGA and GTEx databases from GEPIA (see URLs). **(B)** Kaplan-Meier plots of overall survival rate of PDAC patients in TCGA database from GEPIA by *WTAPP1* RNA level (N = 178, HR = 1.6) (see URLs). **(C)** Distribution of *WTAPP1* RNA in cytoplasm and nucleus of PDAC cells with *U6* and *GAPDH* as markers. **(D)** Existence of *WTAPP1* RNA in SW1990 and Capan-2 cells detected by Northern blotting analysis. 28S and 18S rRNAs were served as loading controls. **(E)** Copy number per cell of *WTAPP1* RNA in PDAC cell lines. **(F)** UniProt human protein profile of 20 PDAC lines in Cancer Cell Line Encyclopedia (CCLE) identified no peptides matching *WTAPP1* ORFs. **(G)** Western blot assays of cells with ectopic expression of FLAG- tagged full length *WTAPP1*. MYC (FLAG-tagged) was used as a positive control and lncRNA without coding potential, *WSPAR*, was used as a negative control. **(H)** Ribosome sedimentation analysis of *β-ACTIN*, *XIST* and *WTAPP1* from PDAC cells. Cell lysates were fractionated by sucrose gradient centrifugation. Data are mean ± SEM from 3 independent RT-qPCR determinations.

Deng et al_Supplementary Figure 2

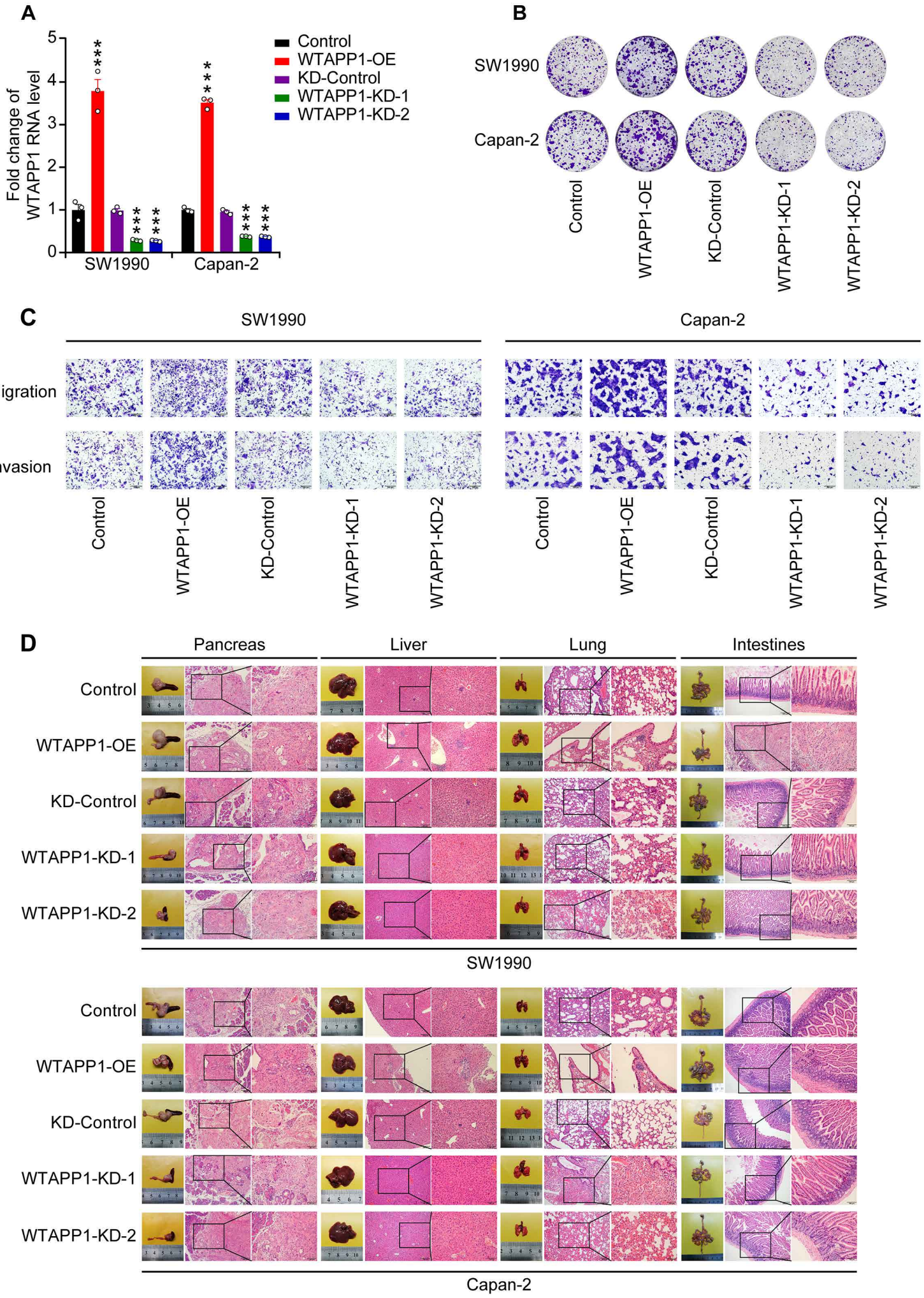

Supplementary Fig. S2 Additional Figures related to Fig. 2 (A) Overexpression or knockdown of *WTAPP1* in PDAC cells (N = 3). Data are mean ± SEM; ***, $P < 0.001$ of Student's *t*-test. **(B, C)** Effects of *WTAPP1* expression levels on the ability of colony formation **(B)** or migration and invasion **(C)** of PDAC cells. Scale bars, 200 µm. **(D)** Histopathological images (H&E staining) the pancreas, liver, lung and intestines from mice transplanted with PDAC xenograft in the pancreas. Scale bars, 200 µm and 100 µm.

Deng et al_Supplementary Figure 3

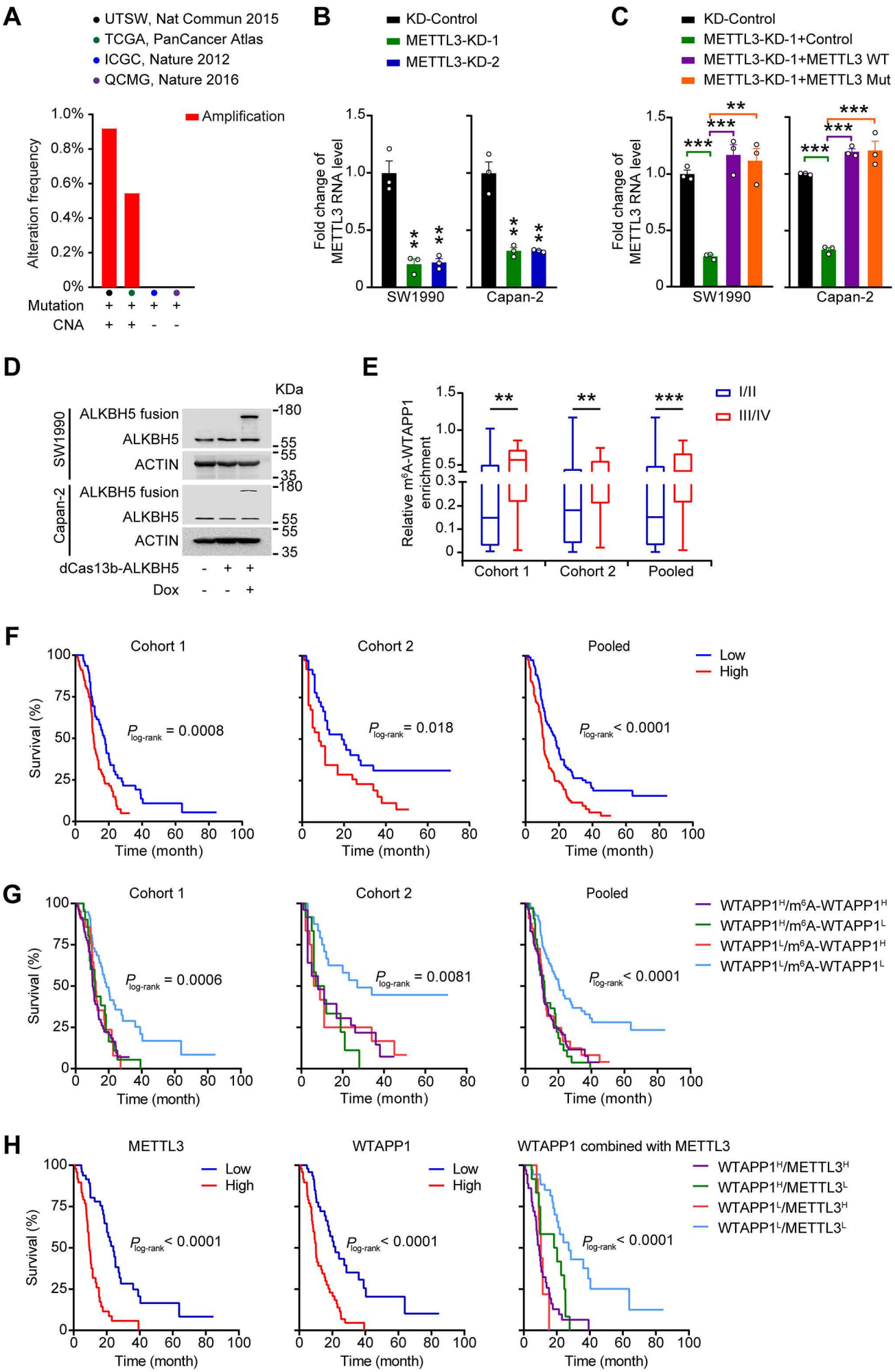

Supplementary Fig. S3 Additional Figures related to Fig. 3 (A) Genomic alterations including mutations and copy number alterations of *WTAPP1* in PDAC tissues derived from different datasets. **(B)** *METTL3* RNA levels in SW1990 and Capan-2 cells transfected with empty vector or vector containing *METTL3* siRNA. **(C)** *METTL3* RNA levels in *METTL3* knockdown cells transfected with vectors containing wild type *METTL3* or its mutant. **(D)** Expression of dCas13b-ALKBH5 fusion protein in PDAC cells with or without doxycycline induction, measured by Western blotting using ALKBH5 antibody. **(E)** m^6A-*WTAPP1* RNA levels are significantly higher in Stage III/IV PDAC than that in stage I/II PDAC in patients of cohort 1 (N = 158), cohort 2 (n = 73) and combined sample (N = 231). **(F)** Kaplan-Meier estimates of overall survival time in PDAC patients from two cohorts and combined sample by m^6A-*WTAPP1* level in tumor (Cohort 1, HR = 1.79, 95% CI = 1.25–2.57, Low, N = 79 and High, N = 79; Cohort 2, HR = 1.84, 95% CI = 1.08–3.12, Low, N = 36 and High, N = 37 and combined sample, HR = 1.79, 95% CI = 1.33–2.41, Low, N = 115 and High N = 116). **(G)** Kaplan-Meier estimates of combined overall survival by *WTAPP1* and m^6A-*WTAPP1* levels in PDAC patients of two cohorts and combined sample (Cohort 1: *WTAPP1*^{high}/m^6A-*WTAPP1*^{high} , N = 58; *WTAPP1*^{high}/m^6A-*WTAPP1*^{low}, N = 21; *WTAPP1*^{low}/m^6A-*WTAPP1*^{high}, N = 21; *WTAPP1*^{low}/m^6A-*WTAPP1*^{low}, N = 58; Cohort 2: *WTAPP1*^{high}/m^6A-*WTAPP1*^{high}, N = 25; *WTAPP1*^{high}/m^6A-*WTAPP1*^{low}, N = 12; *WTAPP1*^{low}/m^6A-*WTAPP1*^{high}, N = 12 and *WTAPP1*^{low}/m^6A-*WTAPP1*^{low}, N = 24 and Cohort 3: *WTAPP1*^{high}/m^6A-*WTAPP1*^{high}, N = 83; *WTAPP1*^{high}/m^6A-*WTAPP1*^{low}, N = 33 and *WTAPP1*^{low}/m^6A-*WTAPP1*^{high}, N = 33; *WTAPP1*^{low}/m^6A-*WTAPP1*^{low}, N = 82) **(H)** Kaplan-Meier estimates of overall survival by *WTAPP1* or *METTL3* level in PDAC in 96 patients from Cohort 1 (METTL3: Low, N = 48 and High, N = 48; WTAPP1: Low, N = 48 and High, N = 48) and overall survival by METTL3 and WTAPP1 levels in 96 patients from Cohort 1: *WTAPP1*^{high}/*METTL3*^{high}, N = 36; *WTAPP1*^{high}/*METTL3*^{low}, N = 12; *WTAPP1*^{low}/*METTL3*^{high}, N = 12 and *WTAPP1*^{low}/*METTL3*^{low}, N = 36). Data in **(E)** are displayed in min to max boxplot and the difference was tested using Mann-Whitney test. Data in **(B, C)** are mean ± SEM from 3 independent RT-qPCR and the difference was examined by Student's *t*-test. **, $P<0.01$ and ***, $P<0.001$.

Deng et al_Supplementary Figure 4

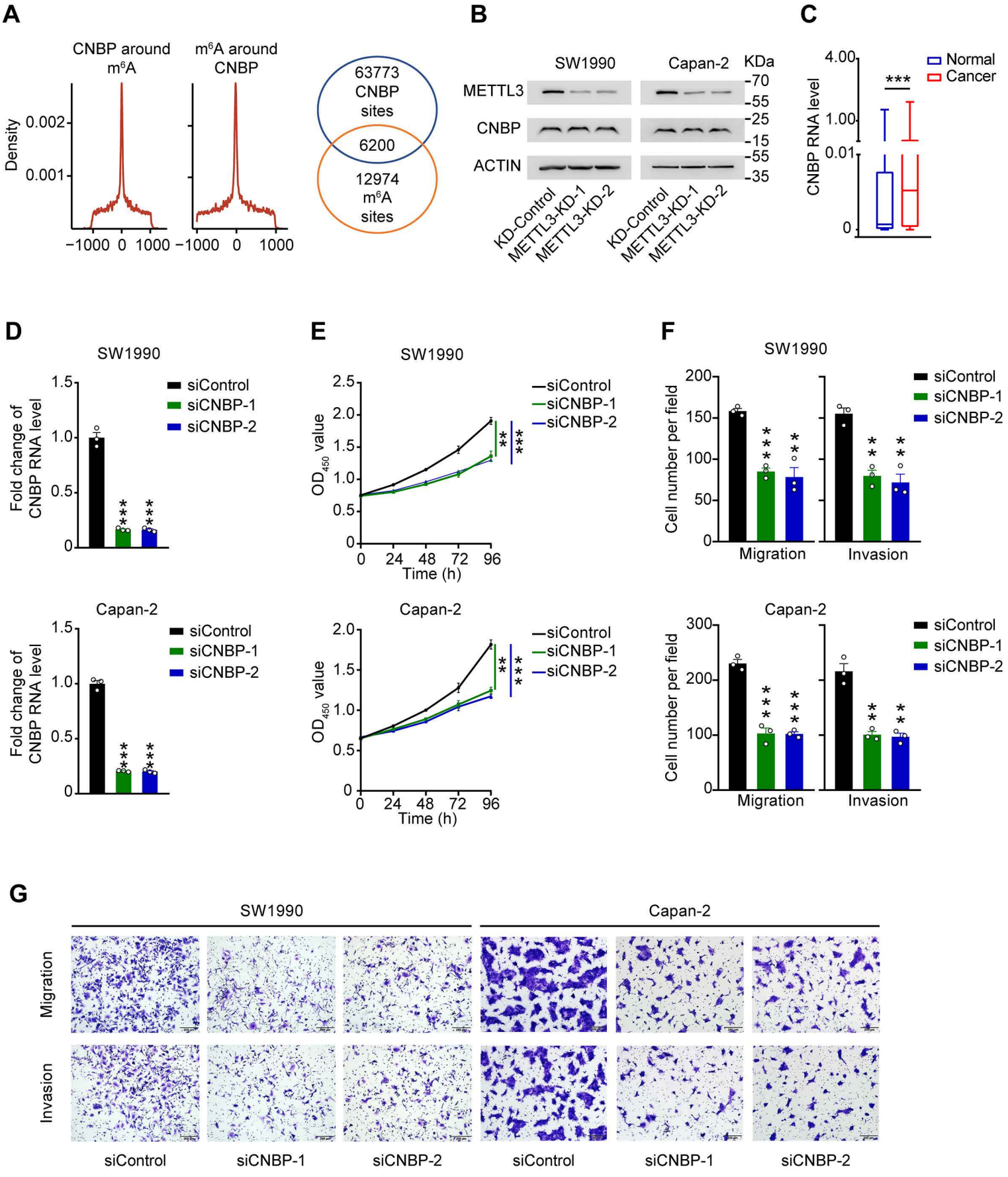

Supplementary Fig. S4 Additional Figures related to Fig. 4 (A) Intensity of CNBP binding centering m^6A residues and m^6A CLIP signal centering CNBP binding sites (*left panel*) and Venn diagram showing overlap between m^6A residues and CNBP-binding sites (*right panel*). **(B)** Western blotting analysis of CNBP protein expression in PDAC cells with METTL3 knockdown. **(C)** Aberrant overexpression of *CNBP* RNA in surgically removed PDAC compared with corresponding non-tumor tissue samples (N = 158). **(D)** *CNBP* RNA levels in SW1990 and Capan-2 cells transfected with negative control or *CNBP* siRNA. **(E–G)** Effects of *CNBP* silence on PDAC cell proliferation **(E)** and migration or invasion **(F, G)**. Data in **(C)** are displayed in min to max boxplot and the difference was tested using Wilcoxon rank-sum test. Data in **(D–F)** are mean ± SEM from at least 3 independent experiments, and the difference was examined by Student's *t*-test. **, $P<0.01$ and ***, $P<0.001$.

Deng et al_Supplementary Figure 5

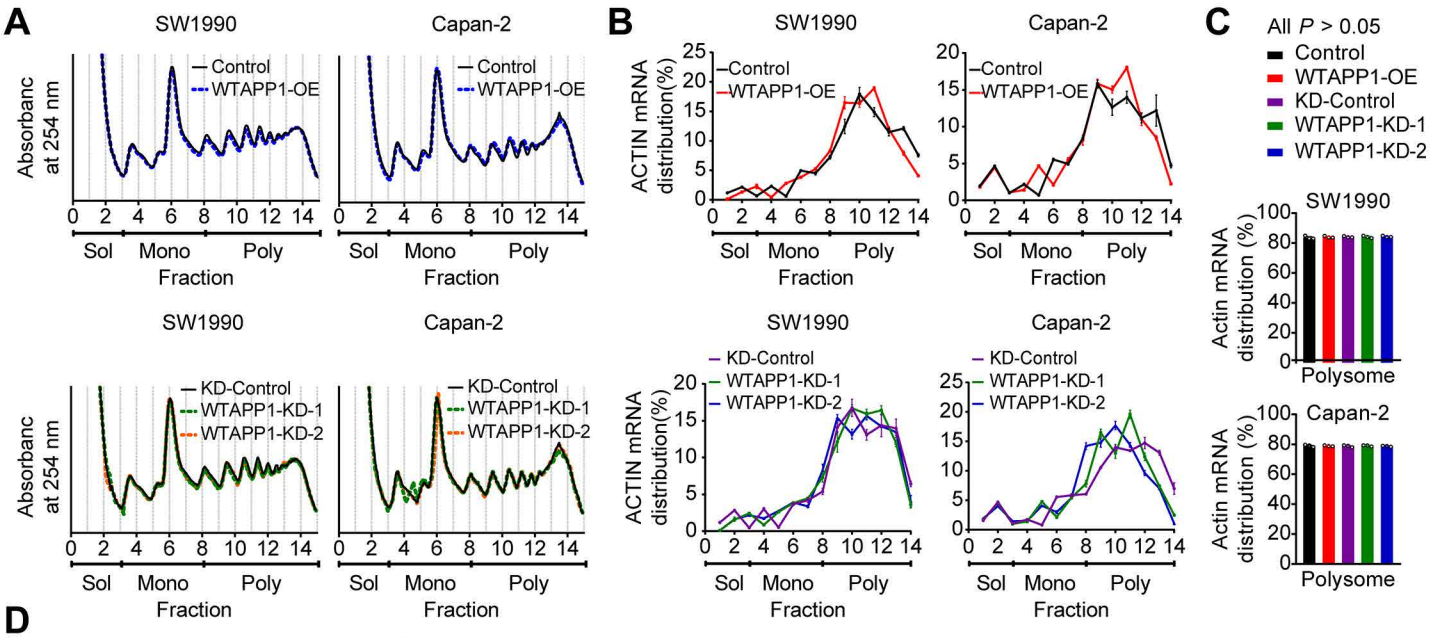

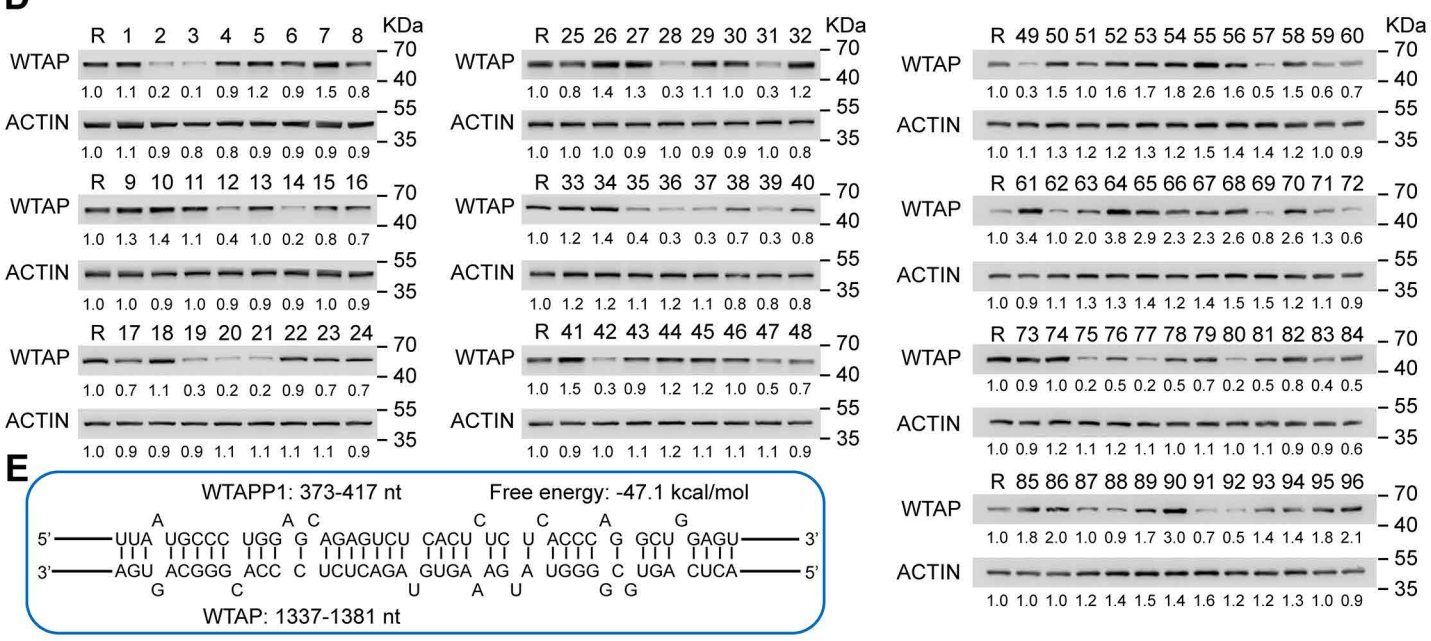

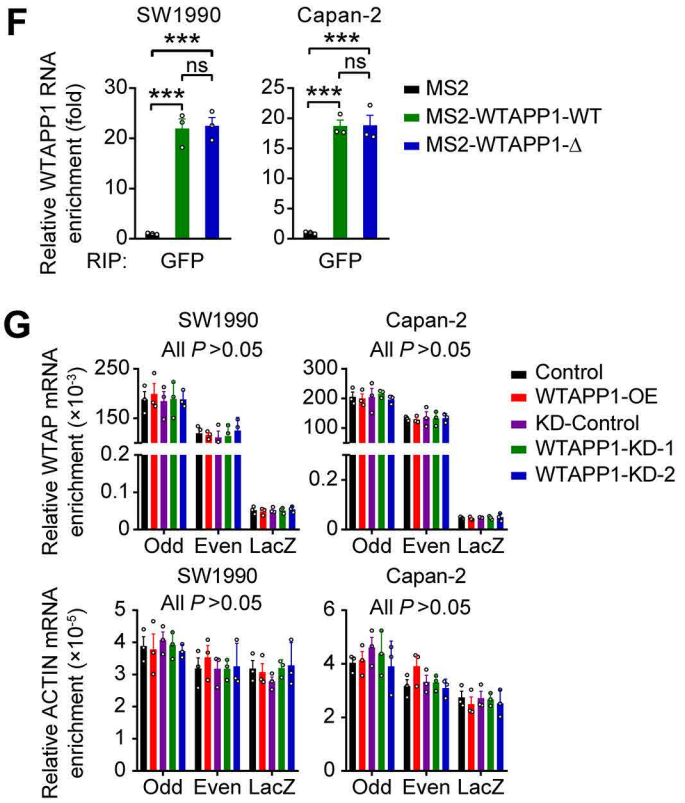

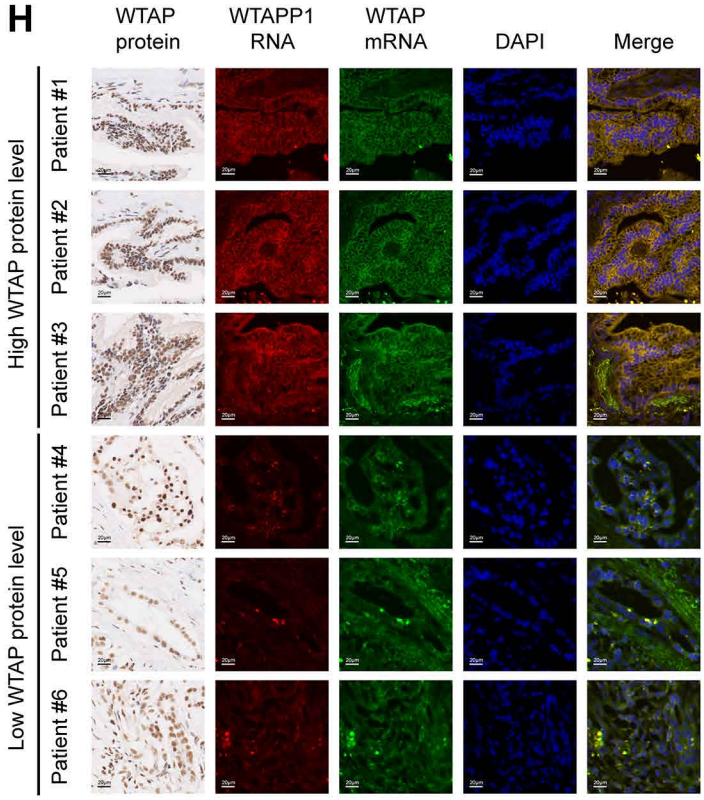

Supplementary Fig. S5 Additional Figures related to Fig. 5 (A) The polysome fractions in PDAC cells with altered *WTAPP1* expression, as shown with profiles of absorbance at 254nm, were separated by sucrose gradient centrifugation. **(B, C)** Polysome fraction analysis in cells by sucrose gradient centrifugation. The level of *β-ACTN* mRNA in each gradient fraction was measured by RT-qPCR and plotted as a percentage of total *β-ACTIN* mRNA level in that sample **(B).** Polysome fractions are shown as bar graph **(C). (D)** Western blot analysis of WTAP protein levels in PDAC tissues (N = 96). R represents the same positive reference sample for loading adjustment on each gel. Each protein band was semi-quantified by gray density and the value for each band is relative to density of corresponding band of R. **(E)** Predicted binding sites of *WTAPP1* RNA and *WTAP* RNA. **(F)** MS2-RIP assays show the levels of *WTAPP1* RNA enriched by anti-GFP antibody in cells with ectopic expression of wild-type *WTAPP1* (MS2-*WTAPP1*-WT) or *WTAPP1* with binding sites deletion (MS2-*WTAPP1*-Δ). **(G)** Results of ChIRP assays using PDAC cell lysate and either *WTAP* mRNA even, odd probe set or LacZ probe set as negative control. Purified RNA was analyzed by RT-qPCR with primers specific for *WTAP* and *β-ACTIN* mRNA. **(H)** Fluorescence in situ hybridization (FISH) of *WTAPP1* and *WTAP* RNA in 6 PDAC samples were grouped by weak or strong Immunohistochemical staining of WTAP proteins. Scale bars, 20 μm. Data are mean ± SEM from 3 independent RT-qPCR analyses and the difference was examined by Student's *t*-test unless specifically indicated.

Deng et al_Supplementary Figure 6

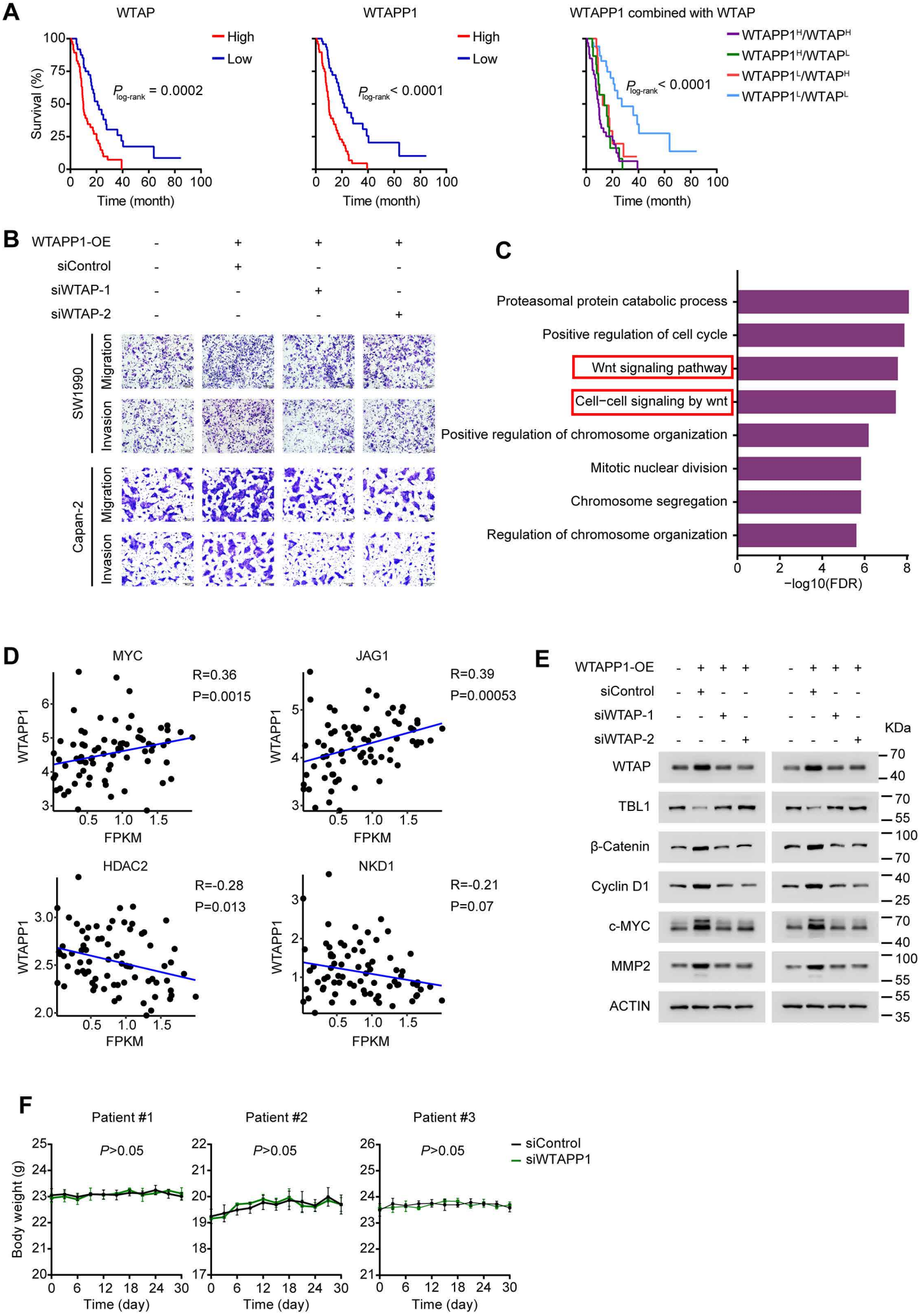

Supplementary Fig. S6 Additional Figures related to Fig. 6 and 7 (A) Kaplan-Meier estimates of overall survival by *WTAPP1* RNA or WTAP protein levels in 96 PDAC patients from Cohort 1 (WTAP: Low, N = 49 and High, N = 47; *WTAPP1*: Low, N = 48 and High, N = 48) and by WTAP and *WTAPP1* levels: *WTAPP1*^{high}/WTAP^{high}, N = 33; *WTAPP1*^{high}/WTAP^{low}, N = 15; *WTAPP1*^{low}/WTAP^{high}, N = 14 and *WTAPP1*^{low}/WTAP^{low}, N = 34). **(B)** Silencing WTAP expression inhibited PDAC cell migration and invasion caused by *WTAPP1* overexpression. Scale bars, 200 μm. **(C)** Gene ontology (GO) analysis of differentially expressed genes identified by RNA sequencing in pancreatic cancer cells with or without *WTAPP1* knockdown (|Foldchange| ≥ 2). **(D)** Correlation between the *WTAPP1* RNA levels and Wnt signaling pathway regulators in PDAC samples from TCGA database. *MYC* and *JAG1* are positive regulators while *HDAC2* and *NKD1* are negative regulators in the Wnt pathway. **(E)** Western blot analysis shows WTAP silence substantially decreased signaling molecules downstream WTAP in cells with *WTAPP1* overexpression. **(F)** Body weight gain (mean ± SEM) of PDX mice treated with or without siWTAPP1. All $P > 0.05$ of Student's *t*-test.